PCCP

PAPER

View Article Online
View Journal | View Issue

Cite this: *Phys. Chem. Chem. Phys.*, 2022, **24**, 24992

Ab initio molecular dynamics investigation of the co-adsorption of iodine species with CO and H_2O in silver-exchanged chabazite

Tarek Ayadi, * Sébastien Lebègue * and Michael Badawi *

In the field of nuclear energy, there is particular interest for the trapping of harmful iodine species (I_2 and CH_3I) that could be released during a nuclear accident, due to their dangereous impact on the human metabolic processes and the environment. Here, the adsorption of these iodine molecules *versus* several inhibitory compounds (CO, H_2O, CH_3Cl and Cl_2) in the silver exchanged chabazite zeolite is studied in detail using *ab initio* molecular dynamics simulations at a realistic temperature and composition. Interestingly, we found that the iodine molecules remain attached to the cations even when the number of water molecules inside the structure is greater than two times the number of cations per cell at T = 413 K. For CO, we found that CH_3I is more perturbed than I_2 by the presence of this inhibitor. Overall, our results indicate that the silver-exchanged chabazite zeolite is a promising candidate to trap iodine species in the case of a severe nuclear accident.

Received 19th May 2022,
Accepted 18th September 2022

DOI: 10.1039/d2cp02267b

rsc.li/pccp

1 Introduction

The safe storage of nuclear waste is an increasingly important topic, especially after the Fukushima nuclear accident. In particular, iodine species are among the most dangereous radioactive compounds that remain of strong interest and concern:[1–3] for public safety, their storage and capture before they reach the environment *via* some leakages of the nuclear containment is crucially important due to their dangerous impact on the human metabolic processes. However, different molecules are released during a nuclear accident which can inhibit the iodine uptake process: it is expected to find large amounts of steam (40–90%) and other gaseous compounds such as CO (0–20%) and chlorinated species (CH_3Cl and Cl_2, with lower concentrations).[4–7] CO mainly comes from the molten core concrete interactions which start after vessel rupture. Chlorinated compounds (CH_3Cl and Cl_2) are produced by fuel fission and possible thermal degradation of cables by pyrolysis.[6,7] On the other hand, we found very low concentrations of radiotoxic iodine (0.1–1 ppm).[8] In this vein, specific filtration devices on the containment venting system are necessary, for instance those based on zeolites, to capture the toxic iodine gas and limit its effect.[9–14]

Zeolites are among the most well-known microporous materials[15–18] that have various applications such as catalysts, cleaners, gas filters and agents for the treatment of nuclear waste due to the presence of structured channels with different dimensions able to capture various types of molecules.[10,12,19,20] Indeed, zeolites show very high thermal and chemical stabilities, and their large structural and compositional varieties[10,12] facilitate the possibility to adjust their properties. Also, the possibility to perform a cationic exchange in the zeolite allows its performance to be tuned by choosing the type of cation to be used to compensate the charge produced in the zeolite structure *e.g.* by the replacement of Si atoms by Al atoms.[18,21,22]

Previous studies have shown that silver exchanged zeolites are optimal for the selective trapping of iodine species, compared to Cu, Na, Pb, Tl and Cd exchanged zeolites.[11,18,23–27] Through an in-depth experimental study on different Ag-exchanged zeolites (faujasites X and Y, mordenite, *BEA, MFI, and FER) to understand the link between the efficiency of iodine trapping and the chemical and structural parameters, Azambre and Chebbi[27] have shown that the formation of AgI precipitates is linked to the performance of zeolites in the capture of the toxic iodine species. Recently, a theoretical study has been carried out by Ayadi *et al.*[28] using density functional theory at T = 0 K to find out the most promising Ag-exchanged zeolitic formulation for the selective trapping of iodine species against several inhibitory molecules (CO, H_2O, Cl_2 and CH_3Cl) in the Ag-exchanged faujasite, mordenite, chabazite and clinoptilolite. They found that CO presents a strong inhibitory effect on the capture of toxic iodine gas for high Si/Al ratios, while Cl_2 presents a strong inhibitory effect for low Si/Al ratios. Overall, a systematic comparison has been performed between

Laboratoire de Physique et Chimie Théoriques (LPCT, UMR CNRS UL 7019), Université de Lorraine, BP 239, Boulevard des Aiguillettes, 54506 Vandoeuvre-lès-Nancy, Cedex, France. E-mail: tarek.ayadi@univ-lorraine.fr, sebastien.lebegue@univ-lorraine.fr, michael.badawi@univ-lorraine.fr

the different zeolites, including the framework topology and the Si/Al ratios, and it was shown that the Ag-exchanged chabazite structure with a Si/Al ratio of 5 is the most promising zeolitic formulation for the capture of the harmful iodine compounds where no inhibitory effect is observed.

Therefore, inspired by these results, we investigate in detail the performance of the silver exchanged chabazite structure with a Si/Al ratio of 5 under more realistic conditions, at T = 413 K and for several molecules at various contents. To this end, we have employed *ab initio* molecular dynamics which is a cutting-edge technique to describe adsorption phenomena under operando conditions.[29–32] During this study, the performance of the chabazite in the adsorption of I_2 and CH_3I *versus* CO, H_2O, Cl_2 and CH_3Cl is examined. Then, the effect of water followed by the effect of CO on the capture of the iodine molecules is investigated. Finally, in order to simulate as realistically as possible the experimental conditions, we have studied the effect of CO together with seven molecules of H_2O on the interactions between iodine compounds and the chabazite structure.

This paper is organized as follows: first, we describe our computational details and the structural model used, then our results for an Ag-chabazite of Si/Al = 5 are presented and discussed with a focus on the effect of the potentially inhibiting molecules (CO, H_2O, Cl_2 and CH_3Cl), followed by the effect of the number of CO and H_2O molecules, and finally we provide the conclusions of our work.

2 Materials and methods

2.1 Computational details

We have performed *ab initio* calculations by means of density functional theory (DFT) with the projector augmented wave (PAW) method[33] as implemented in the Vienna *Ab initio* Simulation Package (VASP).[34] For the exchange and correlation contributions, the Perdew–Burke–Ernzerhof (GGA-PBE) functional[35] was employed with a kinetic energy cutoff of 450 eV for the plane wave basis set. The D2 dispersion correction of Grimme was used to describe dispersion interactions.[36,37] Also, the rev-vdW-DF2 approximation is used where the revised Becke exchange functional (B86R) is adopted for the exchange functional together with the second version of nonlocal vdW-DF.[38] The goal here is to be able to compare the two levels of theory to consolidate our prediction. Regarding the large size of the used unit cell, the calculations were performed with the Γ-point. The convergence parameters were set to 0.02 eV Å^{-1} for the atomic forces and 10^{-6} eV for the total energy.

Using the electronic parameters described above for static DFT relaxations, *ab initio* molecular dynamics simulations (AIMD) were performed over a minimum total simulation time of 120 ps which includes 20 ps for the equilibration period and a time step of 1 fs. To avoid fictitious molecular splitting, the mass of the hydrogen atom is increased to 3 which corresponds to the atomic mass of tritium, which allowed us to set the time-step for integration of the equations of motion to a relatively large value of 1 fs. Using a Nosé–Hoover thermostat,[39,40] the temperature was set to 413 K (temperature reached at the containment). The convergence parameters were set to 10^{-5} for the atomic forces.

The interaction energies for the static DFT calculations between the adsorbate molecules and the chabazite have been calculated using $E_{int} = (E_{zeolite+X} - E_{zeolite} - N_X E_X)/N_X$, where $E_{zeolite+X}$ is the energy of the zeolite with the adsorbed molecules, $E_{zeolite}$ is the energy of the clean zeolite, E_X is the energy of the isolated molecules in the gaseous phase and N_X is the number of molecules inside the zeolite. For AIMD simulations, the internal energy of adsorption was calculated using the equation: $E_{int} = (E_{zeolite+X} - E_{zeolite} - N_X E_X)/N_X$, where $E_{zeolite+X}$, $E_{zeolite}$ and E_X are the average of $E_{zeolite+X}$, $E_{zeolite}$ and E_X, respectively.

2.2 The chabazite model

Chabazite (CHA) is a three dimensional network of SiO_2 composed mainly of four-membered rings (4MRs), double six-ring prisms (6DR) and eight-membered rings (8MRs). The double six-ring prisms (6DR) arranged in layers are connected between each other by tilted four-membered rings (4MRs). The 8MRs function as highly selective doorways with a diameter of 3.8 Å which allow the access to the crystal.[41–43] The pore size of CHA zeolites is about 3.7 Å × 4.2 Å[44] which makes them able to accommodate the molecules studied in this paper, where the longest molecular axes are approximately 2.7 Å and 2.4 Å for I_2 and CH_3I,[26] respectively. Indeed, the size of the chabazite pore is in the same order as those of other zeolites' pores such as mordenite 10.2 Å × 8.4 Å (main channels) and 7.6 Å × 5.7 Å (side channel).[26] Here, we have studied the silver exchanged chabazite with a Si/Al ratio of 5 (Ag-CHA(5) presented in Fig. 1). In this case, the silver loading is about 23.1 wt%. Indeed, recent experimental studies[27] have demonstrated that isolated silver cations can be well inserted into zeolites by cationic exchange even at a high silver loading (up to 23%).

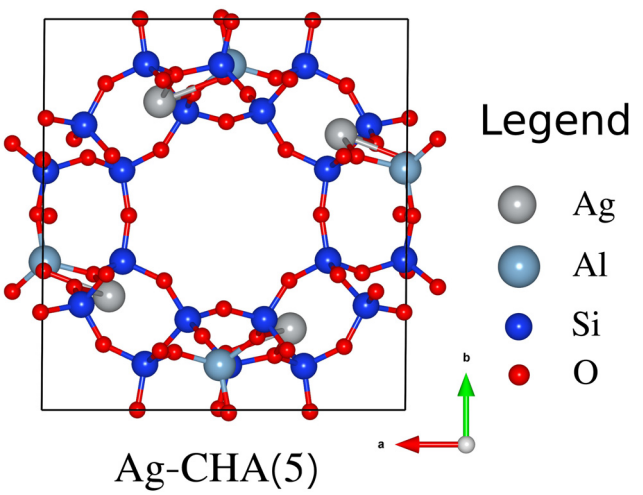

Fig. 1 Structural model of the chabazite (CHA), with a Si/Al ratio of 5, projected along the c direction.

3 Results and discussion

3.1 Adsorption of the single type of molecule

In Table 1, we present our computed interaction energies for CH_3I, I_2, CO, H_2O, CH_3Cl and Cl_2 in the chabazite zeolite at $T = 0$ K and 413 K. According to our calculations, the interaction energy of I_2 and CH_3I is about −206.3 kJ mol^{-1} (−221.7 kJ mol^{-1}) and −170.3 kJ mol^{-1} (−165 kJ mol^{-1}) at $T = 0$ K with PBE + D2 (rev-vdW-DF2), respectively, and these values decrease to −173.6 kJ mol^{-1} and −163.7 kJ mol^{-1}, respectively, at a temperature of 413 K. Also, we found that the iodine species are more strongly bound to the zeolite than H_2O, CO, Cl_2 and CH_3Cl, independently of temperature. At $T = 0$ K, we found with PBE + D2 that the interaction energy of $CH_3I(I_2)$ is more higher (in terms of the absolute value) than those of H_2O, CO, CH_3Cl and Cl_2 by about 47.4 kJ mol^{-1} (83.4 kJ mol^{-1}), 40.2 kJ mol^{-1} (76.2 kJ mol^{-1}), 77.9 kJ mol^{-1} (114 kJ mol^{-1}) and 33.8 kJ mol^{-1} (69.8 kJ mol^{-1}), respectively. The same results are obtained also with the nonlocal functional rev-vdW-D2. At a temperature of 413 K, the CH_3I (I_2) compound is more bound to the chabazite than H_2O, CO, Cl_2 and CH_3Cl, almost with the same quantities of energy obtained at $T = 0$ K which are 44.6 kJ mol^{-1} (54.5 kJ mol^{-1}), 47.4 kJ mol^{-1} (57.3 kJ mol^{-1}), 74.2 kJ mol^{-1} (84.1 kJ mol^{-1}), and 61.8 kJ mol^{-1} (71.1 kJ mol^{-1}), respectively.

Then, we studied the effect of having several molecules of the same type on the capture of the iodine gas and inhibitor compounds (CO and H_2O) at T = 413 K. The results are presented in Fig. 2. We found that the number of molecules has an effect on the adsorption of iodine species, in contrast to CO and H_2O. For the I_2 molecule, the interaction energy decreases from 174 kJ mol^{-1} to 155 kJ mol^{-1}, and then to 147 kJ mol^{-1} when n increases to 2 and then to 3, respectively; for the CH_3I compound, we found that the interaction energy decreases from 164 kJ mol^{-1} to 155 kJ mol^{-1} when n increases to 2, and then to 136 kJ mol^{-1} when n increases to 3. For the inhibitory molecules (CO and H_2O), we found that the effect of the molecule number on the adsorption is rather weak: a decrease by only a few kJ mol^{-1} is obtained with the increase of n to 2 and 3. The different behavior observed between the iodine species and the inhibitory molecules is related to the size of molecules coupled with their adsorption modes in the zeolite. By looking into the adsorption modes, we found that CH_3I is adsorbed on top of two Ag-cations when $n = 1$, and with the increase in the number of molecules, each CH_3I can interact just with a single cation which decreases the interaction energy per molecule (we note that the chabazite contains 4 cations per cell as described above). For I_2, we found that the I atom interacts with more than a single cation on each side of the molecule when $n = 1$, while, with the increase of the number of molecules, each cation in the zeolite can interact with several I_2 molecules, which decreases the interaction energy per molecule. On the other hand, the small size of CO and H_2O allows them to be adsorbed on top of a single cation, independently of the number of molecules, which explains the additive behavior observed in the interaction energy values when n is greater than 1. The effect of the adsorption modes on the decrease of the interaction energy of iodine species is observed also in a previous study on the adsorption of iodine species in the silver-exchanged mordenite zeolite.[14]

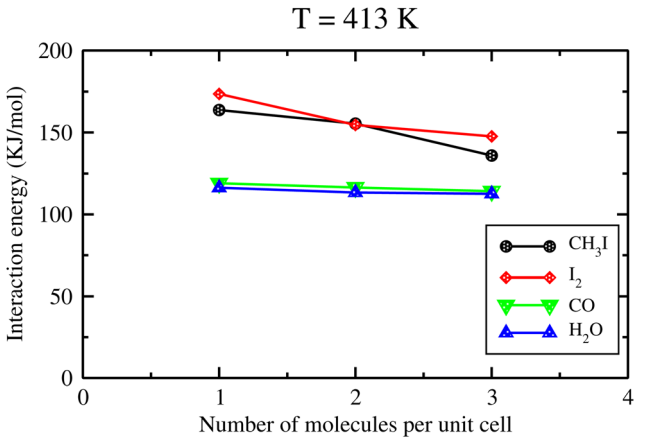

Fig. 2 The variation of the interaction energies per molecule as a function of the number of molecules (n).

3.2 Effect of water molecules

In this section, we study the competitive sorption of iodine species from water in the chabazite structure. Water is one of the most potent inhibitors of the adsorption of harmful iodine species, where its amount ranges between 40% and 90% during a nuclear accident.[4,5,17] We progressively filled the structure by water, molecule by molecule, to study the effect of the number of water molecules on the adsorption of I_2 and CH_3I. Each molecule added, up to 10 water molecules per unit cell which is in the same order as the water quantity (∼7 mmol g^{-1}) adsorbed in the chabazite observed experimentally,[22] with the iodine species is followed by a molecular dynamics simulation of at least 120 ps at 413 K. In Fig. 3, we present the interaction energy per number of water molecules as a function of the number of water molecules. We found that water molecules have a significant effect on the adsorption energies of the iodine species where the interaction energy values per water molecule of CH_3I and I_2 decrease as the number of water molecules increases. For CH_3I, an extreme decrease in the

Table 1 Calculated interaction energies ΔE_{int} (kJ mol^{-1}) for CH_3I, I_2, CO, H_2O, CH_3Cl and Cl_2 in Ag-chabazite, with a Si/Al ratio of 5

		CH_3I	I_2	H_2O	CO	Cl_2	CH_3Cl
$T = 0$ K	PBE + D2	−170.3	−206.3	−122.9	−130.1	−92.33	−136.5
	rev-vdW-DF2	−165	−221.7	−116.3	−130.9	−106.3	−113
$T = 413$ K	PBE + D2	−163.7	−173.6	−119.1	−116.3	−89.5	−115.3

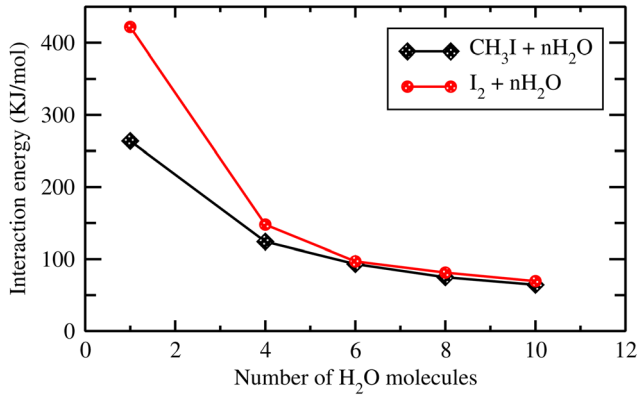

Fig. 3 Interaction energies as a function of number of water molecules.

interaction energy by about 140 kJ mol^{-1} is observed when n increases from 1 to 4, and then, the interaction energy presents a small decrease from 124 kJ mol^{-1} when n = 4 to 93 kJ mol^{-1} when n = 6, then to 75 kJ mol^{-1} when n = 8, and finally to 64.5 kJ mol^{-1} for n = 10. For the I_2 molecule, we also found that the number of water molecules has an effect in the adsorption mechanism, but it is more significant than that observed in the case of CH_3I: first, the interaction energy strongly decreases from 422 kJ mol^{-1} to 148 kJ mol^{-1} when n increases from 1 to 4; second, E_{int} decreases by about 51 kJ mol^{-1} with the increase of n from 4 to 6; and finally, E_{int} presents a small decrease by a few kJ mol^{-1} when n increases to 8, and then to 10. It appears that when n = 1, the iodine molecules are adsorbed on top of more than a single cation, while the water molecule is adsorbed on top of an another single cation; when the number of water molecules ranges between 4 and 10, the iodine molecules are adsorbed on top of a single cation and, in some cases, they shared the same cations with water molecules which decreases the interaction energy and explains the quasi-stability in the energy values per water molecule obtained when n is superior to 1. To confirm our explanation, we present in Fig. 4 the last configurations obtained at t = 120 ps where we observe that the cations are shared between iodine molecules and water, and that the adsorption modes are similar when n ranges between 4 and 10, in contrast to n = 1. To better understand the effect of water on the adsorption of iodine species, we have computed the radial distrubution function (RDF) of the Ag–I distances of Ag–ICH_3 and Ag–I_2 interactions with different numbers of water molecules inside the chabazite structure, see Fig. 4. Without water molecules, the RDFs indicate that the Ag–I distances are about 2.67 Å and 2.65 Å in the case of CH_3I and I_2, respectively. With the addition of a water molecule with the iodine molecules inside the chabazite, the results show that the presence of water has no effect on the Ag–I distance but a small decrease of the peak intensity is observed. This behavior is also observed with the increase of the number of water molecules to 4. On the other hand, the results obtained for CH_3I with n = 6, 8 and 10 present an increase by 0.1 Å for the Ag–I distance, with an appearance of a second weak peak at 3.5 Å for n = 8, and at 4.5 Å for n = 10. This second peak is the result of the movement of CH_3I from one cation to another under the effect of the temperature together with water molecules, while the small increase in the Ag–I distance can be a result of the adsorption of the molecules of water with the iodine molecule on top of the same cations. For the I_2 molecule, we found that the presence of the H_2O molecules also has an effect, depending on the number of molecules, on the interaction of I_2 with the chabazite structure. When n = 1, any effect observed in the Ag–I distance, which is about 2.65 Å, is not surprising because I_2 and water molecules are adsorbed on the top of different cations as presented in Fig. 5. With the increase of the number of water molecules, we found that the Ag–I distance is around 2.7 Å but with a decrease in the principle peak intensity coupled by an increase in the second peak intensity at 4 Å. Also, we can see that the RDF curves are very similar for n ranging between 4 and 10 which is related to similar adsorption modes as presented in Fig. 5. Indeed, we found that the iodine species remain attached to the cations even when the number of water molecules inside the structure is greater than two-fold the number of cations per cell which means that water is not a

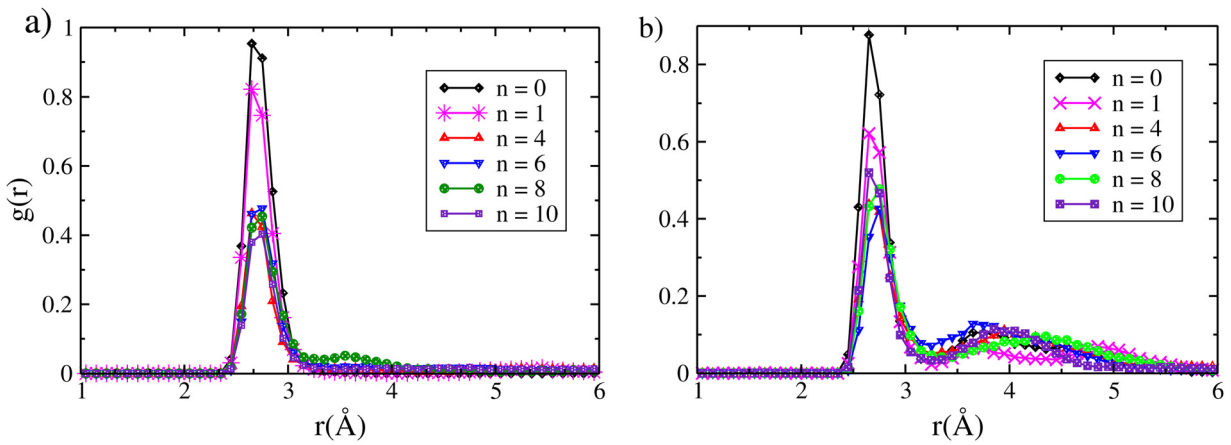

Fig. 4 Radial distribution function of the Ag–I distances of (a) Ag–CH_3I and (b) Ag–I_2 interactions with different numbers (n) of water molecules inside the chabazite structure.

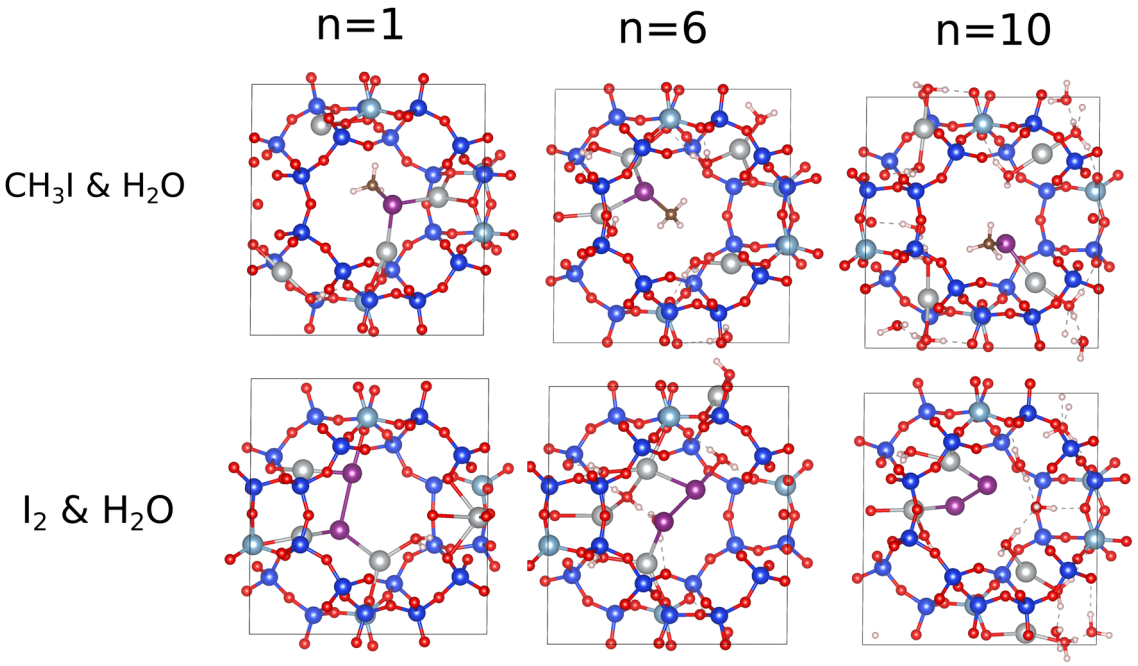

Fig. 5 Adsorption modes of CH_3I (I_2) and water molecules in the chabazite structure.

strong competitive component against iodine species. These findings are very interesting in the case of a nuclear accident and for the scientists in the field of nuclear energy due to the existence of a high amount of water in the nuclear containment, as described above.

3.3 Effect of CO molecules

CO is expected to be one of the most potent inhibitors for the trapping of the toxic iodine molecules, where its quantity varies from 0 to 20% during a nuclear accident.[4,5,17] Here, we aim to investigate the effect of CO on the interaction of iodine species with zeolite where we put an iodine species together with the CO molecule inside the chabazite. AIMD calculations show that the interaction energy of CO and CH_3I is about -257 kJ mol^{-1}, which is less than the sum of the interaction energies of CH_3I and CO adsorbed alone by about 23 kJ mol^{-1}. By looking into the RDF calculations of the Ag–I distance presented in Fig. 6 for CH_3I, we found that the adsorption of CO in the chabazite has a small effect on the Ag–I distance where it increases from 2.65 Å to 2.73 Å, which means that the interaction between CH_3I and the zeolite is weakly disturbed. Otherwise, we found that the interaction energy of I_2 and CO is about -295.7 kJ mol^{-1}, while the sum of the interaction energy of I_2 and CO adsorbed alone is about -289.9 kJ mol^{-1}. Using RDF analysis, we found that the average Ag–I distance is 2.65 Å in the case of I_2, with and without the presence of CO in the zeolite. Here, we observe that CH_3I is more perturbed by the presence of CO than I_2, where the interaction energy decreases by about 23 kJ mol^{-1} coupled with an increase in the Ag–I distance in the case of CH_3I, compared to a decrease in the interaction energy of I_2 by about 5.8 kJ mol^{-1}. Despite the weak effect observed in the case of CH_3I, the iodine species remain in close interaction with

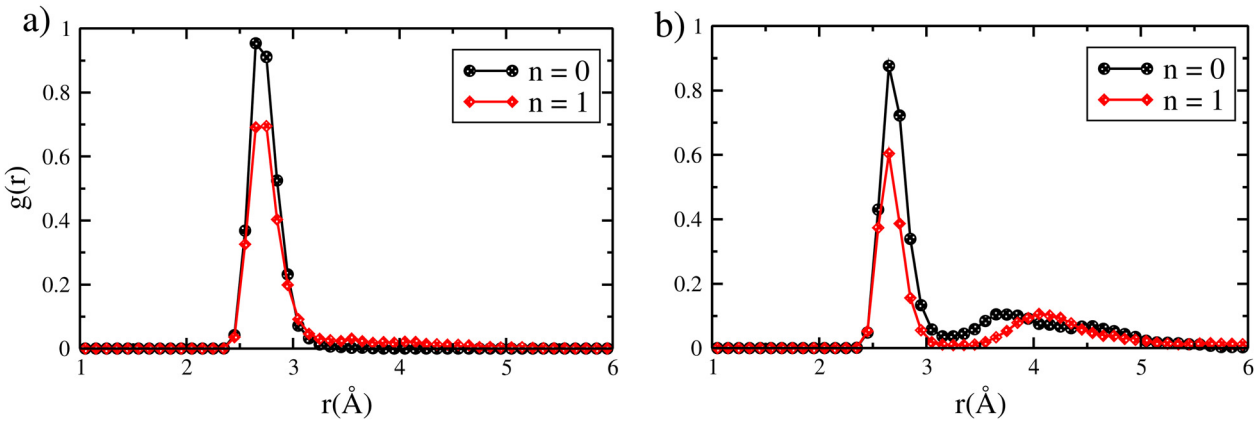

Fig. 6 Radial distribution function of the Ag–I distances of (a) Ag–CH_3I and (b) Ag–I_2 interactions with the CO molecule inside the chabazite structure.

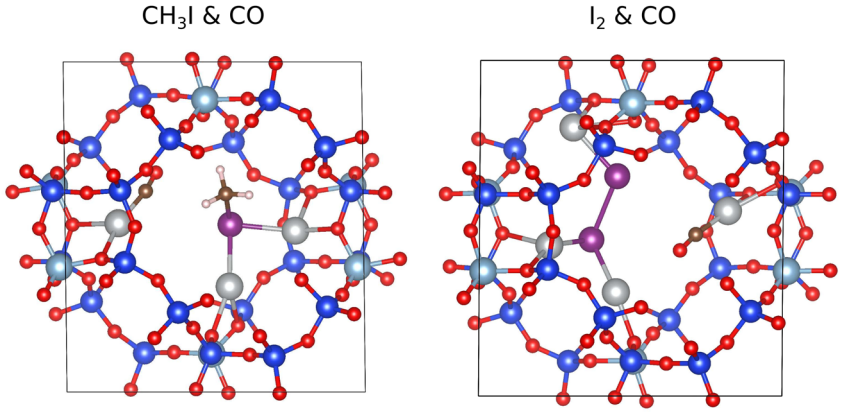

Fig. 7 Adsorption modes of $CH_3I(I_2)$ and CO in the chabazite structure.

cations and no deformation in the framework is observed (see Fig. 7).

3.4 Capture of iodine species from a realistic feed

We now turn to study the competition between the iodine species and two types of inhibitor compounds (H_2O and CO) where we put in the same cage a molecule of iodine species (I_2 or CH_3I) together with seven molecules of water and a molecule of CO. The choice of the number of molecules is related to the amount of water and CO from nuclear waste. Our calculations at 413 K show that the interaction energy of $CH_3I(I_2)$, 7 H_2O and CO is of -670.4 kJ mol^{-1} (-626.3 kJ mol^{-1}) which is less than the sum of the interaction energies of $CH_3I(I_2)$, 7 H_2O and CO adsorbed alone which is about -1113.7 kJ mol^{-1} (-1123.6 kJ mol^{-1}). The RDF calculations of the Ag–I distances for Ag–ICH_3 and Ag–I_2 interactions show that the presence of water and CO, together with iodine species in the same cage, has no significant effect in the interaction mechanism (see Fig. 8). We found that the mean peak is around 2.8 Å for Ag–CH_3I and is around 2.7 Å for the I_2 molecule with and without the presence of the inhibitor molecules. With the addition of inhibitor molecules (CO and 7 H_2O), we observe the appearance of a second peak at 3.5 Å which corresponds to a movement of the iodine species observed during the molecular dynamics simulations. As the chabazite contains 4 cations, the iodine species have the possibility to move from one cation to another one with temperature. Also, we found that the second peak is more intense with the presence of CO in the case of CH_3I. These observations show that CH_3I is more perturbed than I_2 by the presence of CO as observed in our previous work for faujasite at 0 K.[28]

4 Conclusion

Using *ab initio* molecular dynamics simulations at $T = 413$ K, we have investigated the adsorption mechanism of toxic iodine molecules (CH_3I and I_2) against several inhibiting molecules (H_2O, CO, CH_3Cl and Cl_2) in the Ag-exchanged chabazite with a Si/Al ratio of 5. We found that this chabazite presents a good performance in the capture of the iodine gas where the smallest difference in the interaction energy between the iodine species and the inhibiting molecule is about 20 kJ mol^{-1}. Then, we studied the effect of water molecules on the adsorption of CH_3I and I_2: we found that a large decrease in the interaction energies is obtained in the presence of H_2O, in contrast to the Ag–I distance where an increase of 0.1 Å is observed in the

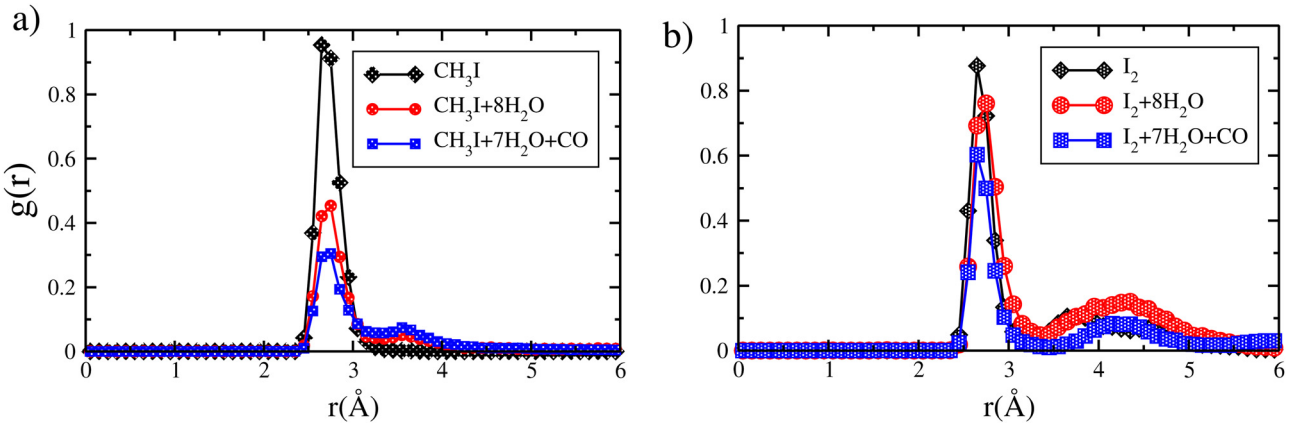

Fig. 8 Radial distribution function of the Ag–I distances of (a) Ag–CH_3I and (b) Ag–I_2 interactions with the H_2O and CO molecules inside the chabazite structure.

extreme case. Also, we studied the effect of CO on the trapping of iodine species where we found that I_2 is less perturbed by the presence of CO compared to CH_3I. Finally, the effect of CO and H_2O together on the adsorption of iodine species was investigated: we have shown that there is a small effect in the interaction between CH_3I and the zeolite where an increase is observed for the Ag–I distance.

Conflicts of interest

There are no conflicts of interest to declare.

Acknowledgements

This work was granted access to the HPC resources of TGCC under the allocations 2021-A0100810433 and A0120810433 provided by GENCI-EDARI and was supported by the French research program ANR-11-RSNR-0013-01 called MiRE (Mitigation of Iodine Releases in the Environment).

Notes and references

1 J. R. Brian, D. V. John, M. S. Denis, S. M. John and L. J. James, *J. Nucl. Mater.*, 2016, **470**, 307–326.
2 A. J. González, *Health Phys.*, 2007, **93**, 571.
3 M. Chebbi, B. Azambre, C. Monsanglant-Louvet, B. Marcillaud, A. Roynette and L. Cantrel, *J. Hazard. Mater.*, 2021, **409**, 124947.
4 L. E. Herranz, T. Lind, K. Dieschbourg, E. Riera, S. Morandi, P. Rantanen, M. Chebbi and N. Losch, OECD REPORT-RN: 47070575, 2013, 2846.
5 D. Jacquemain, S. Guentay, S. Basu, M. Sonnenkalb, L. Lebel, H.-J. Allelein, B. Liebana, B. Eckardt and L. Ammirabile, OECD Report-RN: 45089842, 2014, 174.
6 J. Foit, *Nucl. Eng. Des.*, 1997, **170**, 73–79.
7 A. Auvinen, R. Zilliacus and J. Jokiniemi, *Nucl. Technol.*, 2005, **149**, 232–241.
8 M. Chebbi, B. Azambre, L. Cantrel, M. Huvé and T. Albiol, *Microporous Mesoporous Mater.*, 2017, **244**, 137–150.
9 J. Jolley and H. Tompkins, *Appl. Surf. Sci.*, 1985, **21**, 288–296.
10 K. W. Chapman, P. J. Chupas and T. M. Nenoff, *J. Am. Chem. Soc.*, 2010, **132**, 8897–8899.
11 L. N. Rastunov, E. P. Magomedbekov, A. V. Obruchikov and L. A. Lomazova, *At. Energy*, 2011, **110**, 68.
12 T. M. Nenoff, M. A. Rodriguez, N. R. Soelberg and K. W. Chapman, *Microporous Mesoporous Mater.*, 2014, **200**, 297–303.
13 S. U. Nandanwar, K. Coldsnow, V. Utgikar, P. Sabharwall and D. Eric Aston, *Chem. Eng. Sci.*, 2016, **306**, 369–381.
14 H. Jabraoui, E. Hessou, S. Chibani, L. Cantrel, S. Lebègue and M. Badawi, *Appl. Surf. Sci.*, 2019, **485**, 56–63.
15 M. Kitamura, K. Funabashi, M. Kikuchi, H. Yusa, Y. Fukushima and S. Horiuchi, *Trans. Am. Nucl. Soc.*, 1978, **30**, https://www.osti.gov/biblio/6537164.
16 D. F. Sava, M. A. Rodriguez, K. W. Chapman, P. J. Chupas, J. A. Greathouse, P. S. Crozier and T. M. Nenoff, *J. Am. Chem. Soc.*, 2011, **133**, 12398–12401.
17 S. Chibani, M. Chebbi, S. Lebègue, L. Cantrel and M. Badawi, *Phys. Chem. Chem. Phys.*, 2016, **18**, 25574–25581.
18 M. Chebbi, S. Chibani, J.-F. Paul, L. Cantrel and M. Badawi, *Microporous Mesoporous Mater.*, 2017, **239**, 111–122.
19 V. Van Speybroeck, K. Hemelsoet, L. Joos, M. Waroquier, R. G. Bell and C. R. A. Catlow, *Chem. Soc. Rev.*, 2015, **44**, 7044–7111.
20 E. R. Vance and D. K. Agrawal, *J. Mater. Sci.*, 1982, **17**, 1889.
21 G. D. Pirngruber, P. Raybaud, Y. Belmabkhout, J. Čejka and A. Zukal, *Phys. Chem. Chem. Phys.*, 2010, **12**, 13534–13546.
22 Y. Luo, H. H. Funke, J. L. Falconer and R. D. Noble, *Ind. Eng. Chem. Res.*, 2016, **55**, 9749–9757.
23 R. T. Jubin, Report Number: ORNL/TM-10477, 1988.
24 B. S. Choi, G. I. Park, J. H. Kim, J. W. Lee and S. K. Ryu, *Adsorption*, 2001, **7**, 91.
25 Q. Cheng, Z. Li, T. Chu, W. Yang, Q. Zhu, D. He and C. Fang, *J. Radioanal. Nucl. Chem.*, 2015, **303**, 1883.
26 S. Chibani, M. Chebbi, S. Lebègue, T. Bucko and M. Badawi, *J. Chem. Phys.*, 2016, **144**, 244705.
27 B. Azambre and M. Chebbi, *ACS Appl. Mater. Interfaces*, 2017, **9**, 25194–25203.
28 T. Ayadi, M. Badawi, L. Cantrel and S. Lebègue, *Mol. Syst. Des. Eng.*, 2022, **7**, 422–433.
29 S. Tan, C. Wang, Y. Foucaud, M. Badawi, H. Guo, K. Sun, G. Yang and S. Mintova, *Microporous Mesoporous Mater.*, 2022, **336**, 111853.
30 F.-X. Coudert and D. Kohen, *Chem. Mater.*, 2017, **29**, 2724–2730.
31 Y. Foucaud, J. Lainé, L. O. Filippov, O. Barrès, W. J. Kim, I. V. Filippova, M. Pastore, S. Lebègue and M. Badawi, *J. Colloid Interface Sci.*, 2021, **583**, 692–703.
32 J. Lainé, Y. Foucaud, A. Bonilla-Petriciolet and M. Badawi, *Appl. Surf. Sci.*, 2022, **585**, 152699.
33 G. Kresse and D. Joubert, *Phys. Rev. B: Condens. Matter Mater. Phys.*, 1999, **59**, 1758.
34 G. Kresse and J. Hafner, *Phys. Rev. B: Condens. Matter Mater. Phys.*, 1993, **47**, 558.
35 J. P. Perdew, K. Burke and M. Ernzerhof, *Phys. Rev. Lett.*, 1996, **77**, 3865–3868.
36 S. Grimme, *J. Comput. Chem.*, 2006, **27**, 1787–1799.
37 T. Bučko, J. Hafner, S. Lebègue and J. G. Ángyán, *J. Phys. Chem. A*, 2010, **114**, 11814–11824.
38 I. Hamada, *Phys. Rev. B: Condens. Matter Mater. Phys.*, 2014, **89**, 121103.
39 S. Nosé, *J. Chem. Phys.*, 1984, **81**, 511–519.
40 W. G. Hoover, *Phys. Rev. A: At., Mol., Opt. Phys.*, 1985, **31**, 1695–1697.
41 C. Paolucci, A. A. Parekh, I. Khurana, J. R. Di Iorio, H. Li, J. D. Albarracin Caballero, A. J. Shih, T. Anggara, W. N. Delgass, J. T. Miller, F. H. Ribeiro, R. Gounder and W. F. Schneider, *J. Am. Chem. Soc.*, 2016, **138**, 6028–6048.
42 M. Abatal, A. R. Ruiz-Salvador and C. H. Norge, *Microporous Mesoporous Mater.*, 2020, **294**, 109885.
43 Y. Guo, T. Sun, Y. Gu, X. Liu, Q. Ke, X. Wei and S. Wang, *Chem. – Asian J.*, 2018, **13**, 3222–3230.
44 M. Lee, S. Hong, D. Kim, E. Kim, K. Lim, J. C. Jung, H. Richter, J.-H. Moon, N. Choi, J. Nam and J. Choi, *ACS Appl. Mater. Interfaces*, 2019, **11**, 3946–3960.